Two-Velocities Hybrid RANS-LES of a Trailing Edge Flow

J.C. Uribe*, N. Jarrin*, R. Prosser* and D. Laurence*+

* *School of Mechanical, Aerospace and Civil Engineering, The University of Manchester, Manchester M60 1QD, UK*
+ *EDF R&D, 6 quai Watier, 78420 Chatou, France*

juan.uribe@manchester.ac.uk

Abstract. The flow around a trailing edge is computed with a new hybrid method designed to split the influences of the averaged and instantaneous velocity fields. The model is first tested on channel flows at different Reynolds numbers and coarse meshes giving good predictions of mean velocities and stresses. On the trailing edge flow the predictions of the hybrid model are compared with those using DES-SST on the same coarse mesh. The results of the hybrid model are close to the reference fine LES in terms of mean velocity and turbulent content.

Key words: RANS, LES, trailing edge, hybrid methods.

1. Introduction

Large Eddy Simulation has been successfully applied to different kinds of flows, but its use in industry has remained scarce mainly due to the large constraint present in the mesh requirements of wall bounded flows, specially at high Reynolds numbers. For such flows, the size of the energy containing structures scales with Re_τ and hence the number of grid points required to resolve accurately the near wall eddies scales approximately with $Re^{1.76}$ [6]. To circumvent this severe near wall requirement, LES can be restricted to the simulation of the outer flow eddies whereas a RANS like eddy viscosity model is used to model the dynamics of the near wall eddies. In recent years, such hybrid methods combining RANS and LES have received increased attention from groups around the world.

In an attempt to ease the computational requirements in wall bounded flows, many approaches have been suggested. One method is to use so-called ”wall functions” to bridge the viscous sublayer and provide a suitable boundary condition for the wall cells [22]. This can range from a log-law approximation [24] to a solution of a system of simplified equations in the near wall region [4].

Another approach is the use of RANS equations near the wall to provide the outer layer with correct information. The main problem of this type of approach is how to connect a statistically averaged flow (RANS) with the instantaneous filtered field (LES). A way to couple the two types of flows is the Detached Eddy Simulation (DES) ([26], [32]) in which the turbulent lengthscale in the RANS equation is switched to a lengthscale based on the mesh filter width in order to reduce the viscosity in the separated region

$$l_{DES} = min(l_{RANS}, C_{DES}\Delta) \tag{1}$$

where l_{DES} is the length scale used in DES, l_{RANS} is the length scale from the RANS model, C_{DES} is a model constant and $\Delta = max(\Delta_x\Delta_y\Delta_z)$ is a length scale based on the grid dimension. The main idea of the DES approach is to solve the attached boundary

layers with a RANS models and the separation region with a LES-like technique. One of the main issues of the DES approach is the fact that in regions near the wall where the grid is refined, the turbulent length scale dictated by the RANS model can become larger than the grid length scale therefore making the model reduce the turbulent viscosity and leading to a "grid induced separation" . A way to reduce the sensitivity to the grid induced separation was formulated by Menter et al. [16] using the blending function of the SST model to "shield" the boundary layer. Originally the DES formulation used the Spalart-Allmaras model, but a range of RANS models have been tested [18]. As its name implies, DES should only be applied for separated flows and when the resolution of near wall fluctuations is required, another approach should be used.

Other approaches are 'zonal', in which a part of the domain is set to be computed using RANS equations and the rest is computed with LES. Davidson and Peng [9] used the $k-\omega$ model in a region near the wall ($y^+ \leq 60$) and a one equation model for the sub-grid stresses in the outer region. The location of the interface was fixed and Neumann boundary conditions were applied for the RANS variables. The results for the channel flows calculations were better than those using pure LES on the same grid, but they showed dependence on the matching plane location. Additionally the velocity profile showed a kink or a sudden acceleration at the interface. Davidson and Peng [9] found that the RANS part does not contain enough turbulent characteristics and therefore the LES region is not fed with the correct information. This led to impose turbulent fluctuations at the interface either from a DNS database [8] or from a synthetic method [7]. By imposing fluctuations, it was found that the channel flow predictions are in much better agreement with DNS than without forcing. Another zonal approach has been developed by Temmerman et al. [30] where continuity of the turbulent viscosity is imposed at the interface. Different RANS models and different locations for the interface have been tested. Using this constraint, the coefficient C_μ is extracted from the interface and then adapted via exponential functions to increase the RANS contribution as the wall is approached. The results for a channel flow simulations at high Reynolds number, although not perfect, were far superior then a standard LES on the same coarse mesh.

Hamba [13] tried coupling a near-wall RANS region with an outer LES by using a lengthscale computed from DNS. The approach resulted in an acceleration of the velocity profile at the interface, which was compared to another approaches where there is a similar effect ([9], [21]).

The direction followed by Abe [1] was based on the blending of the total stress τ_{ij} as a combination of the subgrid stress and the RANS stress. A non-linear eddy viscosity model was used for the calculation of the stresses in both regions, the only difference being that the RANS part was calculated using transport equations for k and ε whereas the LES part used algebraic definitions. The blending function was parameterised by the ratio of the distance to the wall and the grid size.

In the zonal approach, the treatment of the interface has always been of importance for the success of the method since the RANS information does not provide correct turbulent fluctuations. Some ways to deal with this issue are the introduction of backscatter [23], damping the modelled stresses [29], the addition of fluctuations at the LES side of the interface [8] or the use numerical smoothing [33].

2. The hybrid approach

In many hybrid approaches the main problem is how to couple the two different velocity fields used in RANS (statistically averaged) and LES (filtered). This is often done by applying a matching criteria, i.e. same turbulent viscosity at the interface, same kinetic energy or dissipation etc. This poses a problem since these values represent totally different properties of different velocity fields. Instead of using one velocity field to couple RANS and LES, the model presented here attempts to adjust the resolved velocity field with information taken from the averaged velocity field. Many sub-grid models assume that the flow contains an inertial subrange and hence the sub-grid motions can be assumed to be isotropic. This is true only if the grid is small enough so that the anisotropy introduced by the mean shear can be neglected. At high Reynolds numbers, the refinement of the grid becomes too costly, therefore restricting the LES method to low Reynolds numbers flows. As the solid boundary is approached, the mean shear becomes high enough to introduce anisotropy across a diminishing range of scales. It is then necessary for the model to represent at the same time subgrid-scale contributions to the mean shear stress and isotropic dissipation effects. The approach presented herein differs form the previous ones by an attempt to separate these two issues in a way that allows the LES fluctuations to develop deeply in RANS layer without any perturbation on or from the mean flow characteristics. This allows to use coarser near wall meshes in all directions (i.e. very high aspect ratio cells as in classical near-wall RANS grids) while maintaining the turbulent characteristics of a resolved field on the whole domain.

2.1. MODELLING

The instantaneous velocity can be decomposed as

$$U = \langle U \rangle + u' \tag{2}$$

where $\langle U \rangle$ is the averaged velocity and u' is the fluctuating one.

Schumann [24] proposed to split the residual stress tensor into two, one "locally isotropic" part and one "inhomogeneous" part. The isotropic part is proportional to the fluctuating strain and does not affect the mean flow equations but determines the rate of energy dissipation. The inhomogeneous part is proportional to the mean strain and controls the shear stress and mean velocity profile:

$$\tau_{ij}^r - \frac{2}{3}\tau_{kk}\delta_{ij} = \underbrace{-2\nu_r(\overline{S}_{ij} - \langle \overline{S}_{ij} \rangle)}_{\text{locally isotropic}} - \underbrace{2\nu_a \langle \overline{S}_{ij} \rangle}_{\text{inhomogeneous}} \tag{3}$$

where $\langle . \rangle$ denotes ensemble averaging of the filtered equations. The viscosities ν_r and ν_a are based on fluctuating and mean strains. The isotropic part of the residual stress tensor has a zero time mean value. By refining the grid the residual stresses must tend to zero, therefore the inhomogeneous part must have a grid dependence parameter in the turbulent viscosity ν_a. Schumann [24] used a mixing length model for ν_a with the length scale computed as $L = \min(\kappa y, C_{10}\Delta)$, where C_{10} is a constant that is difficult to prescribe for all types of flows. Schumann [24] and Grotzbach and Schumann [11] tried to derive a theoretical value for the constant but they were forced to introduced corrective constants to agree with a range of experiments. Moin and Kim [19] used the same principle of splitting the residual stress but in the mixing length model, they use the spanwise size

of the cell as the length scale. They argue that for the near wall region in a channel flow, the important structures are streaks that are finely spaced on the spanwise direction. Therefore a coarse resolution in the spanwise direction would lead to larger eddies and a thicker viscous sublayer. Sullivan et al. [28] developed a similar approach for planetary boundary layer flows but chose ν_a to match the Monin-Obukhov similarity theory [5]. Baggett [3] used a similar approach to compare two hybrid models, one "Schumann-like" and one "DES-like" but found excessive streamwise fluctuations leading to streaks that were much too large.

In the context of hybrid LES-RANS, a blending function, f_b, can be used to introduce a smooth transition between the resolved and the ensemble averaged turbulence parts. In the present study the total residual stress is written as:

$$\tau_{ij}^r - \frac{2}{3}\tau_{kk}\delta_{ij} = -2\nu_r f_b(\overline{S}_{ij} - \langle\overline{S}_{ij}\rangle) - 2(1-f_b)\nu_a\langle\overline{S}_{ij}\rangle \tag{4}$$

In this way the averaged stress would be:

$$\left\langle \tau_{ij}^r - \frac{2}{3}\tau_{kk}\delta_{ij} \right\rangle = 2(1-f_b)\nu_a\langle\overline{S}_{ij}\rangle \tag{5}$$

which is just the RANS stress. This way the total shear stress would be $2(1-f_b)\nu_a\langle\overline{S}_{ij}\rangle + \langle u'v'\rangle$. It is therefore necessary that the blending function f_b tends to one in the region where $\langle u'v'\rangle$ is resolved correctly and to zero in the region near the wall where the shear stress is under resolved due to the coarse grid. The total rate of transfer of energy from the filtered motions to the residual scales is given by (assuming that $\left\langle \nu_r\overline{S}_{ij}\overline{S}_{ij}\right\rangle \approx \nu_r\left\langle \overline{S}_{ij}\overline{S}_{ij}\right\rangle$ [20])

$$\begin{aligned} -\left\langle \tau_{ij}\overline{S}_{ij}\right\rangle = & \quad 2\left\langle \nu_r f_b(\overline{S}_{ij} - \left\langle\overline{S}_{ij}\right\rangle)\overline{S}_{ij}\right\rangle + 2(1-f_b)\left\langle \nu_a\left\langle\overline{S}_{ij}\right\rangle\overline{S}_{ij}\right\rangle & (6)\\ = & \quad 2f_b\nu_r(\left\langle\overline{S}_{ij}\overline{S}_{ij}\right\rangle - \left\langle\overline{S}_{ij}\right\rangle\left\langle\overline{S}_{ij}\right\rangle) + 2(1-f_b)\nu_a\left\langle\overline{S}_{ij}\right\rangle\left\langle\overline{S}_{ij}\right\rangle & (7)\end{aligned}$$

which shows how the RANS viscosity contributes to dissipation in association with the mean velocity only, i.e. the resolved turbulent stresses are free to develop independently from the RANS viscosity.

For the isotropic viscosity ν_r, Schumann [24] used a model based on the sub-grid energy. Moin and Kim [19] used the standard Smagorinsky [25] model based on the fluctuating strain. Here the later approach is used:

$$\nu_r = (C_s\Delta)^2\sqrt{2s'_{ij}s'_{ij}} \tag{8}$$

$$s'_{ij} = \overline{S}_{ij} - \langle\overline{S}_{ij}\rangle \tag{9}$$

In the frame of unstructured codes, the filter width is taken as twice the cell volume ($\Delta = 2Vol$).

In this study the elliptic relaxation model $\phi - f$ of Laurence et al. [14] is used to calculate the RANS viscosity. This model solves for the ratio $\phi = \overline{v^2}/k$ to compute the turbulent viscosity as:

$$\nu_a = C_\mu\phi kT \tag{10}$$

where $T = \max\left(\frac{k}{\varepsilon}, C_T\sqrt{\frac{\nu}{\varepsilon}}\right)$. Although for the channel flow calculations presented here, there is not much difference in the choice of the RANS models, the aim is to have a

formulation that can be used in complex 3D flows, therefore the elliptic relaxation method seems a suitable choice to account for the wall effects.

The blending function has been parameterised by the ratio of the turbulent length scale to the filter width:

$$f_b = \tanh\left(C_l \frac{L_t}{\Delta}\right)^n \tag{11}$$

Here $C_l = 1$ and $n = 1.5$ are empirical constants. These values were chosen to match the shear stress profile based on channel flow results at $Re_\tau = 395$ with DNS data. When using the $\phi - f$ model (equation 10), the wall distance is not desirable and the blending function can be formulated using $L_t = \phi k^{3/2}/\varepsilon$. The blending function has been devised to connect the two length scales smoothly so its value is close to zero near the wall and one far from it. Similar functions have been used in other hybrid approaches (See Abe [1], Hamba [12] or Speziale [27]). Although the function in equation 11 is totally empirical, it has been tested for a range of Reynolds numbers and grids and gave satisfactory results (not presented here). The function allows a higher contribution from the LES part as the grid is refined. Different coefficients have been used in the optimisation of the blending function, but the results are not greatly affected and anyway are always better than standard LES on the same mesh. In equation (4) the averaged velocity has been calculated as a running average with an averaging window of about 10 times the eddy turnover time. Although it is possible also to use plane averaged in the case of the channel flow, this was not done in order to keep the formulation applicable for 3D flows where no plane averaging is possible. In all computations shown here, a finite volume code *Code_Saturne*[2] has been used with a second order time advancing scheme.

3. Channel Flows

Channel flow computations have been carried out at different Reynolds numbers on the same domain, a box of dimensions [0,6.4],[0,2],[0,3.2]. Here only few of the simulations are shown. For the channel flow at $Re_\tau = 395$ the coarsest mesh used has 40x40x30 cells (denoted C1). In figures 1 and 2 the resulting velocity and shear stress profiles for a standard Smagorinsky model and the hybrid model can be seen. The mesh is too coarse for a standard LES to capture all the small scales and therefore the shear stress is underpredicted, which in turn, produces an overestimation of the velocity magnitude. The hybrid model successfully blends the average shear stress and with the resolved one to produce the correct magnitude and therefore a better prediction of the velocity profile. The normal stresses can be seen in figure 3. The usual behaviour of overestimating the streamwise normal stress on coarse meshes by LES is corrected by the hybrid model. For higher Reynolds numbers the results have a similar trend. In figure 4 the velocity profiles are shown for different Reynolds number with coarse meshes. All the velocity profiles follow the log-law. A comparison can be made with the DES method that, eventhough is not designed to compute attached flows, is capable of retaining some fluctuating content in coarse meshes. In figure 5 the profiles of mean velocity are shown for the hybrid model and DES-SST at $Re_\tau = 4000$ on a 64x80x64 mesh. The DES computation produces a shift in the velocity profile which is not uncommon to different hybrid methods [21]. This is due to the sudden change from RANS to LES where the RANS model probably damps excessively fluctuating motions near the interface, which are then not able to develop sufficiently rapidly to build up the shear stress through resolved eddies only, up to the

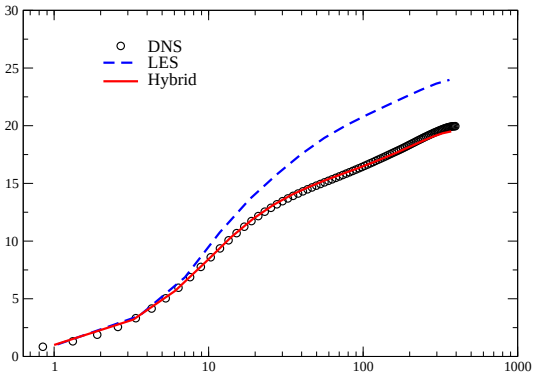

Figure 1. Velocity profile at $Re_\tau = 395$

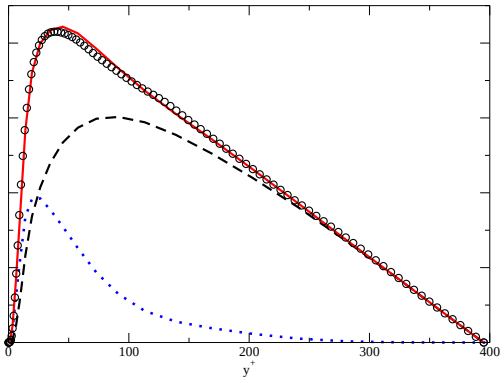

Figure 2. Shear stress at $Re_\tau = 395$

Figure 3. Normal stresses at $Re_\tau = 395$

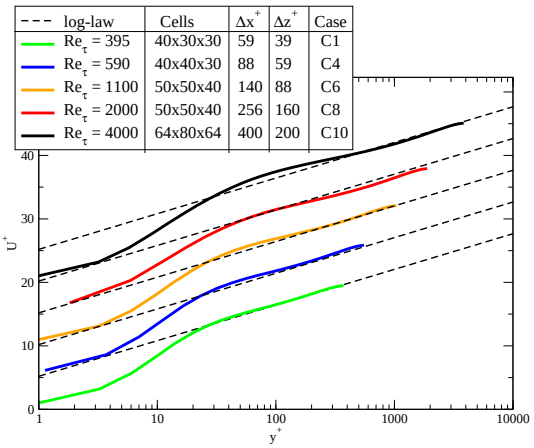

Figure 4. Velocity profiles at different Reynolds numbers.

level of stress fully modeled in the RANS layer. On the other hand the hybrid model retains the turbulent content that can be resolved by the coarse mesh. The instantaneous streamwise velocity contours on a plane at $y^+ = 200$ can be seen in figures 6 and 7 where it is clear the the DES model produces the "superstreaks" [23] which are much larger than what the grid can support.

4. Trailing Edge Computations

In the present study, we performed various hybrid simulations of the flow past an axisymmetric bevelled trailing edge. The geometry is described in detail in [35]. The Reynolds number based on the free stream velocity U_∞ and the hydrofoil chord, is 2.15×10^6. The trailing edge tip angle is 25 degrees. Simulations were performed over the rear-most 38% of the hydrofoil chord with inlet conditions discussed below. The inlet Reynolds numbers based on the local momentum thickness and boundary layer edge velocity are 2760 on the lower side and 3380 on the upper side. These values were obtained from an auxiliary RANS calculation although some questions remain about their fidelity as mentionned in [34] and [35]. The computational domain is $0.5h \times 41h \times 16.5h$ where h denotes the hydrofoil thickness. The grid was coarsened from $1536 \times 96 \times 48$ cells (claimed to be sufficient for a well resolved LES by Wang and Moin [35]) to $512 \times 64 \times 24$ cells. The

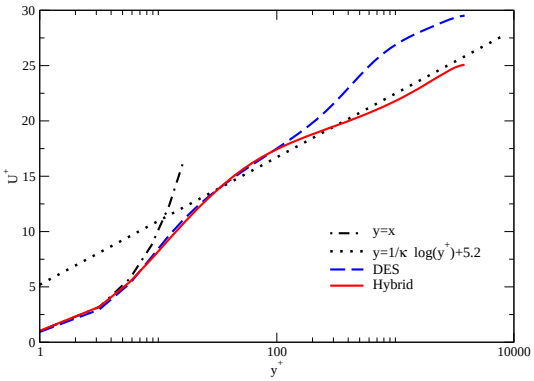

Figure 5. Velocity profiles at $Re_\tau = 4000$

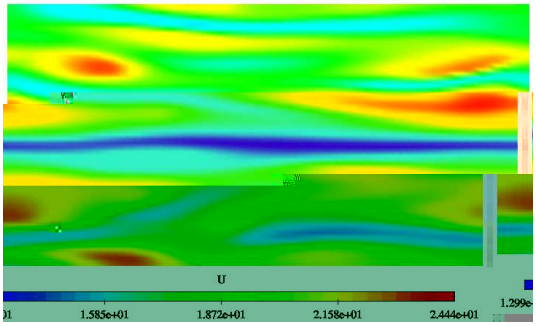

Figure 6. Instantaneous streamwise velocity contours. DES

Figure 7. Instantaneous streamwise velocity contours. Hybrid model

mesh has 192 cells in the streamwise direction on the wing both on the lower and on the upper side and 64 cells in the wake. The maximum grid spacing in wall unit is $\Delta z^+ = 110$ in the spanwise direction and $\Delta x^+ = 230$ in the streamwise direction. The mesh spacing in the streamwise direction is kept constant along the trailing edge when it is refined in the fine LES of Wang and Moin [35] ($\Delta z^+ = 55$ and $\Delta x^+ = 60$). The minimum grid spacing in the wall normal direction is about $\Delta y^+ = 2$.

The boundary conditions at the inlet are taken from Wang and Moin [35] using the following procedure. First, an auxiliary RANS calculation is conducted in a domain enclosing the entire strut. The resulting mean velocities, accounting for the flow acceleration and circulation associated with a lifting surface, are used as the inflow profiles outside the boundary layers on both side of the strut. Originally two RANS simulations were performed using the $v^2 - f$ turbulence model of Durbin [10] and the Menter [17] SST model. In the present study the SST profiles have been used. The two turbulence model produce a noticeable difference in the velocity overshoot (undershoot) outside the upper (lower) boundary layer. SST results are associated with a smaller mean circulation, which is thought to promote trailing edge separation. Within the turbulent boundary layers the time series of inflow velocities are generated from two separate LES calculations of flat-plate boundary layers with zero pressure gradient, using the method described by Lund et al. [15

strut. The top and bottom boundaries are placed far away from the strut to minimise the impact of the imposed symmetry boundary condition. At the downstream boundary a standard exit boundary condition is applied. This case has been treated with dynamic wall models by Wang and Moin [36] and with similar methods in Tessicini et al. [31].

Two simulations using the same mesh are presented here. One with DES using the SST model as the RANS background model. The blending function F_1 is used to avoid grid induced separation (see [16] for details). The second simulation is done with the hybrid method presented above. Velocity profiles and rms streamwise velocity fluctuations profiles are available from the fine LES [35] at locations of $x/h = -0.625$, -1.125, -1.625, -2.125, -3.125 on the aerofoil and at $x = 0, 0.5, 1, 2$ and 4 in the wake ($x/h = 0$ is located at the trailing edge). Figure 8 shows the absolute velocity ($\sqrt{U^2 + V^2}$) profiles at the five stations on the aerofoil. The hybrid model presents a better agreement with the reference LES. It can be seen how the DES separates earlier and by the station at $x/h = -1.125$ there is a strong recirculation which is not present in the reference LES. The hybrid model predicts a slightly earlier separation but closer to the reference value. The turbulent content is also better predicted by the hybrid model as it can be seen from figure 9. The DES simulation does not sustain the fluctuations from the inlet and by the time the flow reaches the station at $x = -3.125$, the resolved fluctuations are very small. This is the normal behaviour of DES in an attached boundary layer, since it is designed to be used in massively separated flows.

In general the structures predicted by DES are larger than what the hybrid model predicts.The structures are better resolved than with the DES approach because in the hybrid model the resolved stresses can develop independently from the RANS viscosity, i.e. the model associates the RANS viscosity with the mean flow only and links the resolved scale dissipation to the LES viscosity only (as shown in equation (7)). This can be seen in figures 10 and 11 where the isosurfaces of fluctuating streamwise velocity are shown (+0.05 in red, -0.05 in blue). This is mainly due to the way in which each approach treats the boundary layer. DES uses RANS in a zone much larger near the wall, solving much of the boundary layer. On the other hand, the hybrid only uses full RANS in a zone very close to the wall and then it has a transition zone where both approaches contribute via different velocity fields. The blending function contours can be seen in figure 14. In figure 15 the zones where the two different length scales are used on the DES simulation can be seen. The red region region represents where the DES acts in LES mode, i.e. where the turbulent scale ($k^{3/2}/\varepsilon$) is larger that the filter length scale ($C_s\Delta$). In DES, the zone close to the wall is solved in RANS mode, therefore damping the fluctuations, whereas the hybrid model resolves the structures dictated by the size of the mesh, and introduces the effect of the wall via the averaged velocity. Although DES is acting in LES mode in the separated region, as it is designed to do, it is possible that the coarse resolution of the grid does not allow for a good resolved LES. Therefore a finer grid would probably lead to better results but this issue needs to be investigated further.

In figure 12 the streamwise velocity profiles at the wake can be seen. Due to the better representation of the separated region by the hybrid model, the velocity profiles are in a better agreement than the DES. The rsm fluctuations can be seen in figure 13 where it can be seen that the levels are similar, although the spectral content is most certainly very different (as seen from figures 10 and 11) and this is important in aero-acoustic applications.

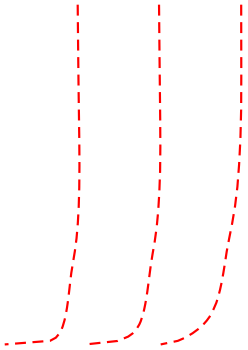

Figure 8. Velocity profiles over the aerofoil

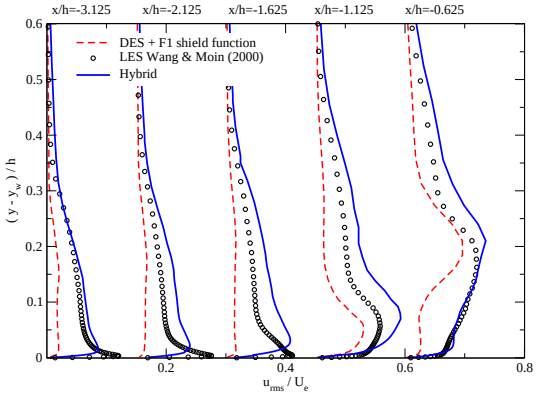

Figure 9. u_{rms} profiles over the aerofoil

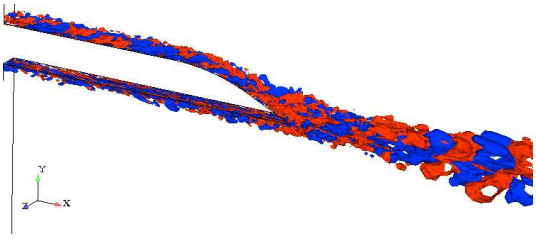

Figure 10. Iso-contours of u', hybrid model

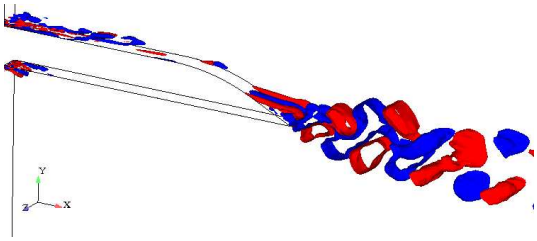

Figure 11. Iso-contours of u', DES model

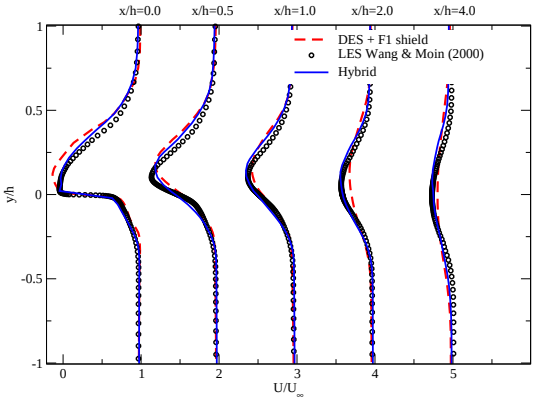

Figure 12. Velocity profiles at the wake

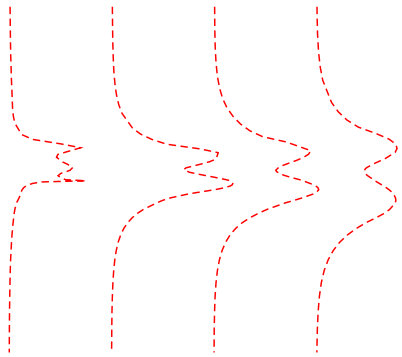

Figure 13. u_{rms} profiles at the wake

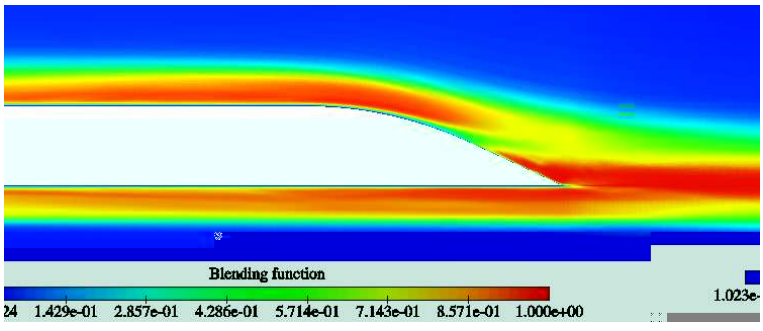

Figure 14. Blending function contours for the hybrid model

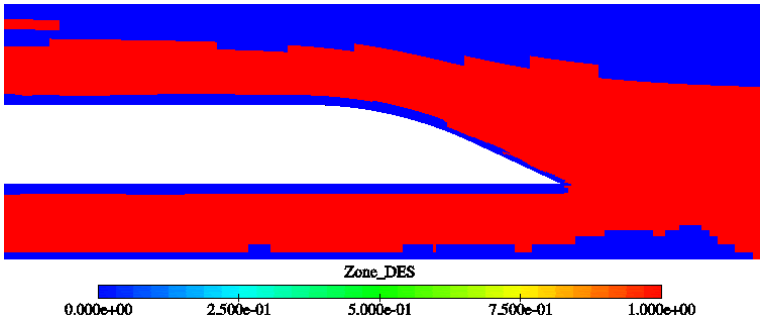

Figure 15. LES and RANS zones on DES simulation

5. Conclusions

A new hybrid method has been presented based on splitting the contributions from the averaged and fluctuating velocity fields. The method performs well in channel flows where the boundary layer is attached and on the separated flow over a trailing edge. The method has been compared with the DES method which is not designed to reproduce the behaviour of attached boundary layers. In the case of the separated flow around a trailing edge, the DES method behaves in LES mode in the separated region but is found to be not turbulent enough predicting a early separation from the curved surface. On the other hand, the hybrid method is capable of sustaining fluctuating behaviour only limited by the size of the cells. Although the mesh is too coarse to be able to reproduce the small structures, the model successfully includes the near wall effect on mean strain via the mean velocity field, allowing a separation of dissipative effects. This makes the model predict better separation and mean quantities compared to the DES simulation. There are many issues to investigate such as the sensitivity of the model to different meshes and different blending functions but the results obtained here are encouraging.

Acknowledgements

This work was financed by the DESider project (Detached Eddy Simulation for Industrial Aerodynamics) which is a collaboration between Alenia, ANSYS-AEA, Chalmers University, CNRS-Lille, Dassault, DLR, EADS Military Aircraft, EUROCOPTER Germany, EDF, FOI-FFA, IMFT, Imperial College London, NLR, NTS, NUMECA, ONERA, TU Berlin, and UMIST. The project is funded by the European Community represented by the CEC, Research Directorate-General, in the 6th Framework Programme, under Contract No. AST3-CT-2003-502842.

References

[1] K Abe. A hybrid LES RANS approach using an anisotropy-resolving algebraic turbulence model. *International Journal of Heat and Fluid Flow*, 26:204–222, 2005.

[2] F. Archambeau, N. Mechitoua, and M. Sakiz. A finite volume method for the computation of turbulent incompressible flows - industrial applications. *International Journal on Finite Volumes*, 1(1), 2004.

[3] J.S Baggett. On the feasibility of merging LES with RANS for the near-wall regions of attached turbulent flows. In *Annual research Briefs*, pages 267–276. Center for turbulence research, Stanford, CA, 1998.

[4] E. Balaras, C. Benocci, and U. Piomelli. Two-layer approximate boundary conditions for large eddy simulations. *AIAA Journal*, 34:1111–1119, 1996.

[5] J. A. Businger, J. C. Wyngaard, Y. Izumi, and E. E. Bradley. Flux-profile relationships in the atmospheric surface layer. *Journal of Atmospheric Science*, 28:181–189, 1971.

[6] D. Chapman. Computational aerodynamics development and outlook. *AIAA journal*, 17:1293–1313, 1979.

[7] L. Davidson and M. Billson. Hybrid RANS-LES using synthetized turbulence for forcing at the interface. In P. Neittaanmäki, T. Rossi, S. Korotov, E. Oñate, J. Périaux, and D. Knörzer, editors, *ECCOMAS*, 2004.

[8] L. Davidson and S. Dahlström. Hybrid LES-RANS: An approach to make LES applicable at high reynolds number. *International journal of computational fluid dynamics*, 19:415–427, 2005.

[9] L. Davidson and S.-H. Peng. Hybrid RANS-LES: A one equation sgs model combined with a $k-\omega$ model for predicting recirculating flows. *International journal of numerical methods in fluids*, 43: 1003–1018, 2003.

[10] P.A. Durbin. A reynolds stress model for near-wall turbulence. *Journal of Fluid Mechanics*, pages 465–498, 1993.

[11] G. Grotzbach and U. Schumann. Direct numerical simulation of turbulence velocity -pressure, and temperature fields in channel flows. In *Symposium on turbulent shear flow*, pages 18–20, 1977.

[12] F. Hamba. An attempt to combine large eddy simulation with the $k-\varepsilon$ model in a channel flow calculation. *Theoretical and computational fluid dynamics*, 14:323–336, 2001.

[13] F. Hamba. A hybrid RANS LES simulation of turbulent flows. *Theoretical and computational fluid dynamics*, 16:387–403, 2003.

[14] D. Laurence, J.C. Uribe, and S. Utyuzhnikov. A robust formulation of the v2-f model. *Flow, Turbulence and Combustion*, 73:169–185, 2004.

[15] T. Lund, X. Wu, and D. Squires. Generation of turbulent inflow data for spatially-developing boundary layer simulations. *Journal of Computational Physics*, 186:652–665, 1998.

[16] F. Menter, M. Kuntz, and R. Langtry. Ten years of industrial experience with the SST model. In K. Hanjalić, Y. Nagano, and M. Tummers, editors, *Turbulence, Heat and Mass Transfer 4*, 2003.

[17] F. R. Menter. Zonal two-equation $k-\omega$ turbulence models for aerodynamic flows. *AIAA Journal*, page 2906, 1993.

[18] C. Mockett, U. Bunge, and F. Thiele. Turbulence modelling in application to the vortex shedding of stalled airfoils. In M. Rodi, W. nd Mulas, editor, *Engineering Turbulence Modelling and Experiments 6*, pages 617–626, 2005.

[19] P. Moin and J. Kim. Numerical investigation of turbulent channel flow. *Journal of fluid mechanics*, 118:341–377, 1982.

[20] F. Nicoud, J. S. Baggett, P. Moin, and W. Cabot. Large eddy simulation wall-modeling based on suboptimal control theory and linear stochastic estimation. *Physics of fluids*, 13:2968–2984, 2001.

[21] N.V. Nikkitin, F. Nicoud, B. Wasistho, K.D. Squires, and P. Spalart. An approach to wall modelling in large eddy simulations. *Physics of fluids*, 10:1629–1632, 2000.

[22] U. Piomelli and E. Balaras. Wall-layer models of large eddy simulation. *Annual review of Fluid Mechanics*, 34:349–374, 2002.

[23] U. Piomelli, E. Balaras, E. Pasinato, K.D. Squire, and P. Spalart. The inner-outer later interface in large eddy simulation with wall layer models. *Interntional journal of heat and fluid flow*, 23:538–550, 2003.

[24] U. Schumann. Subgrid scale model for finite difference simulations of turbulent flows in plane channels and annuli. *Journal of computational physics*, 18:676–404, 1975.

[25] J. Smagorinsky. General circulation experiments with the primitive equations: I the basic equations. *Monthly Weather Review*, 91:99–164, 1963.

[26] P. Spalart, W. Jou, M. Strelets, and S. Allmaras. Comments of feasibility of les for wings, and on a hybrid RANS/LES approach. In *International Conference on DNS/LES, Aug. 4-8, 1997, Ruston, Louisiana.*, 1997.

[27] C.G. Speziale. Turbulence modeling for time-dependant RANS and VLES: a review. *AIAA Journal*, 26:179–184, 1998.

[28] P. Sullivan, J. McWilliams, and C. Moeng. A subgrid-scale model for large eddy simulation of planetary boundary layer. *Boundary layer methodology*, 71(247–276), 1994.

[29] L. Temmerman and M. Leschziner. A priori studies of near wall RANS model whithin a hybrid LES/RANS scheme. In Rodi W. and Fueyo N., editors, *Engineering turbulence modelling and experiments, 5*, pages 371–326, 2002.

[30] L. Temmerman, M. Hadẑiabdić, M. Leschziner, and K. Hanjalić. A hybrid two-layer URANS-LES approach for large eddy simulation at high Reynolds numbers. *International journal of heat and fluid flow*, 26:173–190, 2005.

[31] F. Tessicini, L. Temmerman, and M. A. Leschziner. Approximate near-wall treatments based on zonal and hybrid ransles methods for les at high reynolds numbers. *International Journal of Heat and Fluid Flow*, 27:789799, 2006.

[32] A. Travin, M. Shur, M. Strelets, and P. Spalart. Detached-eddy simulation past a circular cylinder. *Flow Turbulence and Combustion*, pages 393–313, 1999.

[33] P. Tucker and L. Davidson. Zonal $k-l$ based large eddy simulations. *Computational fluid dynamics*, 33:267–287, 2004.

[34] M. Wang. Progress in les of trailing-edge turbulence and aeroacoustics. In *Annual research briefs*. ky7s9pTD[(k32(t)-23TD[(F1 9.96 Tf 135.46 0 TpTD[(k3dh[28])]TJh.)-24d[28])]TCA50(1997.)]TJ ET BT 11.34 -135.434